Metastatic timing and genetic heterogeneity in the evolution of a pancreatic neuroendocrine tumor

Tang, Xia; Shao, Yue; Yi, Xin; Newey, Paul; Li, Dewei; Ding, Keyue

Published in:
American Journal of Gastroenterology

DOI:
10.14309/ajg.0000000000001004

Publication date:
2021

Licence:
CC BY-NC

Document Version
Peer reviewed version

Metastatic timing and genetic heterogeneity in the evolution of a pancreatic neuroendocrine tumor

Xia Tang, MS[1,*], **Yue Shao, MS**[2,*], Xin Yi, PhD[3], Paul J. Newey, PhD[4], Dewei Li, PhD[2,$], Keyue Ding, PhD[1,$], and Gastrointestinal Cancer Evolution Study Group

[1]*Department of Bioinformatics, School of Basic Medicine, Chongqing Medical University, Chongqing, China;* [2]*Department of Hepatobiliary Surgery, The First Affiliated Hospital of Chongqing Medical University, Chongqing, China;* [3]*Geneplus-Beijing Institute, Beijing, China;* [4]*Division of Molecular and Clinical Medicine, Ninewells Hospital and Medical School, University of Dundee, Dundee, United Kingdom*

*Authors share co-first authorship; [$]Authors share co-senior authorship

#: Corresponding authors

Keyue Ding, PhD, E-mail: ding.keyue@igenetics.org.cn; or Dewei Li, MD, E-mail: lidewei406@sina.com

Word count: 498

Informed patient consent

The study was approved by the Institutional Review Board (IRB) of the First Affiliated Hospital of Chongqing Medical University. Written informed consent was obtained from the patient.

Conflicts of interest

P.J.N. has received speaker fees from IPSEN. The authors report no other conflicts of interest.

Author Contributions

D.L. and Y.S. prepared the samples; X.Y. generated sequencing data, X.T. and K.D. performed data analysis; P.J.N. contributed to data interpretation; X.T. and K.D. wrote the manuscript with input from P.J.N. and D.L.; and D.L. and K.D. designed the project.

Acknowledgment

The Gastrointestinal Cancer Evolution Study Group include Liujun Jiang, Liang Chen, Zixin Chen, and Lei Xiang, Department of Hepatobiliary Surgery, The First Affiliated Hospital of Chongqing Medical University, Chongqing; Xinmei Wang, Department of Pathology, School of Basic Medicine, Chongqing Medical University, Chongqing; Fajin Lv, Department of Radiology, The First Affiliated Hospital of Chongqing Medical University, Chongqing; Shasha Bian and Bingtao Hao, Medical Genetic Institute of Henan Province, Henan Provincial Key Laboratory of Genetic Diseases and Functional Genomics, Henan Provincial People's Hospital, Zhengzhou, Henan; and Yanfang Guan, and Rongrong Chen, Geneplus-Beijing Institute, Beijing.

Funding

K.D. and D.L. is funded by the National Natural Science Foundation of China (No.81672780 and 81470898). K.D. is also supported by the program of Artificial Intelligence in Medicine from Chongqing CSTC (ZHYX2019004). P.J.N. holds a Scottish Senior Clinical Fellowship funded by the Chief Scientist Office (CSO)/NHS Research Scotland (NRS) and the University of Dundee [SCAF/15/01].

Pancreatic neuroendocrine tumors (PanNET) account for 1-3% of all pancreatic cancers and are frequently diagnosed at a stage at which distant metastases are evident[1]. Although recent studies[2] have identified driver genes implicated in PanNET development, the molecular events underlying tumor evolution and metastases remain unknown. To gain insight into these processes, we undertook whole-exome sequencing of 12 asynchronously-collected tumor samples from a single PanNET patient over a ~13-year window.

The patient, a 54-year-old male, presented with a ~25×24mm mass in the pancreatic tail and a metastatic lesion in the right lobe of the liver, which was initially misdiagnosed as pancreatic ductal adenocarcinoma. Over the disease course, the patient underwent six surgeries and multiple rounds of chemotherapy (Figure 1a). Details of clinical treatment together with supplementary methods, notes, figures, and tables are provided online (http://www.igenetics.org.cn/project/PanNET/). The pathological diagnosis was revised 9-years after the initial surgery to that of a well-differentiated PanNET (G2, Ki67=3%, Figure 1b; online Figure S1a).

The primary tumor revealed a very high mutation burden (84/MB), a sign of hypermutability[3] (online Figure S1b) and single base substitution (SBS) signature analysis supported defective DNA repair processes (online Figure S1c). Strikingly, this hypermutation phenotype was not observed in any of the synchronous or metachronous metastases. Somatic variants in known PanNET driver genes including *MEN1* (p.Tyr77fs*42, NP_570716), *TSC2* (p.His1860Cysfs*58, XP_005255584.1) and *DAXX* (p.Pro284Arg, NP_001356132.1) were observed in all tumor samples (Figure 1c), consistent with their established roles in tumorigenesis. The patient was also noted to

harbor a rare germline missense *TSC2* variant (p.Arg1369Gln, NP_000539), associated with aberrant mTOR signaling *in vitro* (online Figure S1d-e). Notably, the patient received the mTOR inhibitor everolimus following the last surgery, associated with disease stability.

Analysis of the clonal and subclonal architecture[4] indicated that the majority of metastatic subclones could be traced back to the primary tumor (Figure 1d). However, the low mutation burden observed in each of the metastases indicated that the acquisition of metastatic potential and cancer progression was not a late-event dependent on the hypermutation observed in the primary tumor (as described in other cancers[4]), but arose independent of this at an earlier timepoint. Furthermore, somatic trunk variants in metastasis-associated driver genes (i.e., *TSC2* and *DAXX*), as well in metastasis-specific variants in extracellular matrix genes further support such a model. Subsequent phylogenetic analysis revealed that subclones in the primary tumor (Figure 1e) had both linear and branching seeding patterns. Metastatic spread was dependent on two likely processes; metastatic subclones arising directly from the primary tumor and persisting at clinically occult sites over long periods prior to detection (e.g., dark-blue subclone); and polyclonal seeding events with subsequent metastasis-to-metastasis spread as reported for other cancer types (e.g., purple subclone) (Figure 1f)[4,5].

In summary, this study highlights the utility of temporal and spatial genomic sampling of multiple tumors from a single patient to investigate the genetic factors influencing PanNET disease course, and provides useful insights into tumor initiation,

the potential timing of metastatic seeding, and subsequent metastatic trajectory, which together have potentially important therapeutic implications.

Reference

1. Pipinikas, C. P., Dibra, H., Karpathakis, A., Feber, A., Novelli, M., Oukrif, D., et al. Epigenetic dysregulation and poorer prognosis in DAXX-deficient pancreatic neuroendocrine tumors. Endocr Relat Cancer, 2015;22(3):L13–L18.

2. Scarpa, A., Chang, D. K., Nones, K., Corbo, V., Patch, A.-M., Bailey, P., et al. Whole-genome landscape of pancreatic neuroendocrine tumors. Nature, 2017;543(7643):65–71.

3. Schlesner, M., & Eils, R., Hypermutation takes the driver's seat. Genome Med, 2015;7(1):214–3.

4. Turajlic, S., & Swanton, C., Metastasis as an evolutionary process. Science, 2016;352(6282);167–169.

5. Gundem, G., Van Loo, P., Kremeyer, B., Alexandrov, L. B., Tubio, J. M. C., Papaemmanuil, E., et al. The evolutionary history of lethal metastatic prostate cancer. Nature, 2015;520(7):353–357.

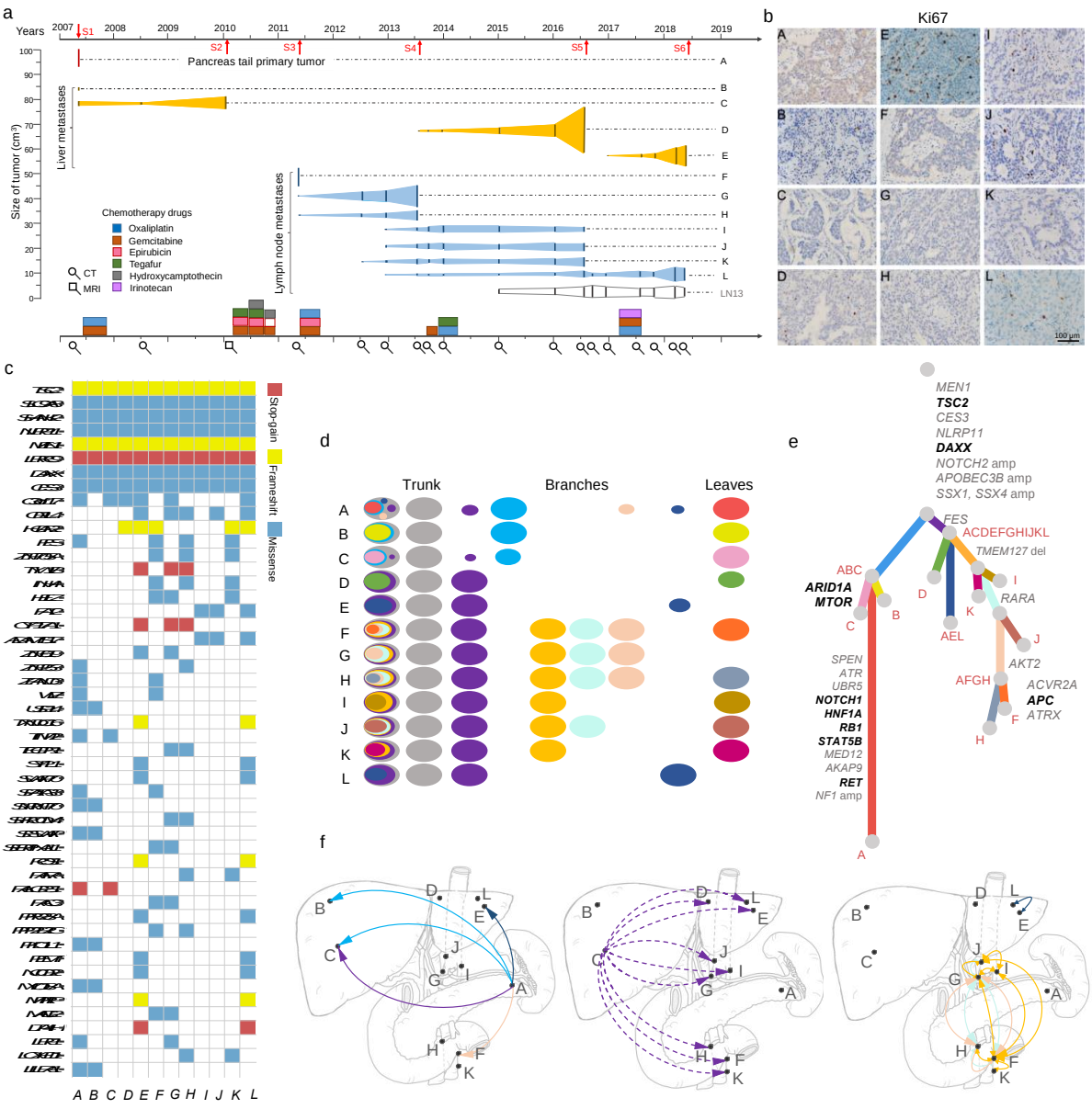

Figure 1 – A PanNET patient with multiple metastatic deposits.

(a) Clinical timeline of the patient's tumor development and disease course. The timeline axis at the top and bottom records the relative timing of the tumor imaging (CT/MRI), surgeries, and therapeutic interventions (online Table S1-S3). The vertical axis provides a scale for the tumor volumes (online Table S2). The primary tumor (A) is represented in red, the liver metastases (B-E) in orange and lymph node metastases (F-

L) in blue. The lymph node LN13 in represented in grey as it is still *in situ* within the patient. The colored bars at the bottom of the panel represent different drugs included in cycles of chemotherapy, with the width corresponding to the therapeutic intervals each combination was used. These sequential rounds of post-operative adjuvant chemotherapy were administered based on the initial misdiagnosis of pancreatic ductal adenocarcinoma.

(b) IHC staining for Ki67 in tumor samples (online Table S4). A Ki67 index of 3% was observed in the primary tumor whilst rates of 2%, 2%, 10%, and 8% were observed in the liver metastases (tumors B, C, D, and E), respectively. No correlation was observed between Ki67 index and tumor mutation burden (p=0.62).

(c) Distribution of non-silent somatic mutations shared between at least two of the tumor samples, i.e., trunk and branch mutations.

(d) Clonal and subclonal architecture of the tumor samples inferred by the distribution of non-silent mutations and selected copy number variants (CNVs) shared between samples (online notes). Tumor clones are represented by ovals, with the likely clonal and subclonal fractions in each sample indicated. Each row represents a sample, with the ovals in the column presented in nested format. The area of each oval represents the estimated proportion of the corresponding subclones. Oval plots are divided into three types: trunk, branch and leaf.

(e) The inferred phylogenetic tree. Branch length is proportional to the number of substitutions. Branches are annotated with sample(s) (i.e. A-L) in which they are present, and with potential driver events assigned to that subclone. Genes represented

in bold are experimentally validated metastases-related genes from the human cancer metastasis database. Amp, amplification; Del, deletion.

(f) Inferred pattern of metastatic seeding events is represented with color-coded arrows. In the left-hand panel, the solid arrows indicate the inferred spread of metastatic clones direct from the primary tumor. The detection of subclones represented by the purple and light blue arrows at tumor C indicate possible polyclonal seeding. Our analysis suggests a potential mechanism represented in the middle panel, in which the purple clone identified in tumor C subsequently undergoes metastasis-to-metastasis seeding (i.e. from tumor C to the remaining metastatic locations, represented by dotted arrows), although it is also possible that the subsequent detection of the purple clone in all samples except sample B, may indicate direct spread from the primary tumor (i.e. tumor clones persisting at these sites over long periods prior to detection) (see online notes for additional details). In the right-hand panel, the double-headed arrows indicate instances in which seeding could be in either direction.